Chiral Spin Liquid Ground State in $YBaCo_3FeO_7$

W. Schweika,[1,2,*] M. Valldor,[3,4] J. D. Reim,[1,5] and U. K. Rößler[3]

[1]*Quantenmaterialien und kollektive Phänomene JCNS-2 & PGI-4, Forschungszentrum Jülich, DE-52425 Jülich, Germany*

[2]*European Spallation Source ESS ERIC, SE-221 00 Lund, Sweden*

[3]*Leibniz-Institut für Festkörper- und Werkstoffforschung IFW Dresden, Helmholtzstraße 20 DE-01069 Dresden, Germany*

[4]*Centre for Materials Science and Nanotechnology (SMN), Department of Chemistry, University of Oslo, P.O. Box 1033 Blindern, N-0315 Oslo, Norway*

[5]*Institute of Multidisciplinary Research for Advanced Materials, Tohoku University, 2-1-1 Katahira, Sendai 980-8577, Japan*

(Received 14 October 2021; revised 18 February 2022; accepted 28 February 2022; published 4 May 2022)

A chiral spin liquid state is discovered in the highly frustrated, noncentrosymmetric swedenborgite compound $YBaCo_3FeO_7$, a layered kagome system of hexagonal symmetry, by advanced polarized neutron scattering from a single domain crystalline sample. The observed diffuse magnetic neutron scattering has an antisymmetric property that relates to its specific chirality, which consists of three cycloidal waves perpendicular to the c axis, forming an entity of cylindrical symmetry. Chirality and symmetry agree with relevant antisymmetric exchanges arising from broken spatial parity. Applying a Fourier analysis to the chiral interference pattern, with distinction between kagome sites and the connecting trigonal interlayer sites of threefold symmetry, the chiral spin correlation function is determined. Characteristic chiral waves originate from the trigonal sites and extend over several periods in the kagome planes. The chiral spin liquid is remarkably stable at low temperatures despite strong antiferromagnetic spin exchange. The observation raises a challenge, since the commonly accepted ground states in condensed matter either have crystalline long-range order or form a quantum liquid. We show that, within the classical theory of magnetic order, a disordered ground state may arise from chirality. The present scenario, with antisymmetric exchange acting as a frustrating gauge background that stabilizes local spin lumps, is similar to the avoided phase transition in coupled gauge and matter fields for subnuclear particles.

DOI: 10.1103/PhysRevX.12.021029

Subject Areas: Condensed Matter Physics
Magnetism

I. INTRODUCTION

Spin liquids do not display a regular magnetic order at temperatures below the energy scale of relevant interactions; geometric frustration, competing interactions, and low dimensionality are common reasons for their apparent lack of order and their richness of exotic properties [1–3]. The combination of frustration and strongly interacting spins creates a common feature of spin liquids, highly correlated spin configurations on a finite length scale and these in astonishing diversity. While the term spin liquid is used in various contexts, a thermodynamic definition implies a state not different from the paramagnetic high-temperature state. Typically, one finds a competition, where couplings allow for several spin orders to coexist. From these degenerate primary modes a distinct ground state is selected, either by an entropic mechanism following the "order by disorder" principle [4] or by weaker magnetic coupling terms, e.g., longer-range exchange or anisotropies. In a three-dimensional magnetic system close to the ground state, spin ordering eventually sets in, either through a classical second-order phase transition or due to hidden multipolar ordering [5], e.g., as the loop order in the garnet $Gd_3Ga_5O_{12}$ [6]. There are exceptions to this, like the spin freezing in spin ice that falls out of equilibrium and avoids the expected, regularly ordered ground state [7]. A mimicry of a spin liquid state and a disordered ground state in $YbMgGaO_4$ [8] is proposed to follow from a background of charge fluctuation disorder. The role of a disordered background seems a convenient speculation to explain a few specific disordered low-temperature spin systems.

*Corresponding author.
W.Schweika@fz-juelich.de

Published by the American Physical Society under the terms of the Creative Commons Attribution 4.0 International license. Further distribution of this work must maintain attribution to the author(s) and the published article's title, journal citation, and DOI.

Advanced polarized diffuse neutron scattering sheds new light on a disordered, but strongly interacting spin system. The experiment reveals strong chirality in the spin correlations of the spin liquid $YBaCo_3FeO_7$, which suggests an alternative route to an amorphous state. Our theoretical analysis shows that long-range spin ordering can be impeded, even in clean magnetic systems, if a set of coexisting spin patterns interacts and is twisted into extended textures. The specific mechanism for this type of frustration derives from antisymmetric exchange couplings and exists in crystals where spatial parity is broken. We propose a generic description of the cooperative spin modes in such a magnetic system that includes a frustrating gauge background and enforces the twisting of spin patterns and generates localized lumps, detected as chiral short-range spin order. These chiral lumps condense into an amorphous state of chiral solitonlike configurations. The prediction is a classical ground state, while the common view only accepts the lack of spatial long-range order in ground states of quantum systems. This particular classical ground state is realized by a number of possible microstates. Therefore, its entropy is finite and larger than zero in accordance with the third law of thermodynamics. The classical chiral spin liquid and its ground state, as described, are different from any of the theoretically postulated chiral quantum spin liquids [9–11].

The studied material is a homolog of the swedenborgite mineral [12]. The mineral has the composition $SbNaBe_4O_7$ and hexagonal, polar, noncentrosymmetric crystallographic symmetry $P6_3mc$, no. 186. Swedenborgites exhibit a vast chemical flexibility [13], including the possibility for magnetic ions to enter the Be sites. The two distinct crystallographic sites constitute a network of trimerized kagome layers connected via trigonal interlayer sites [Fig. 1(a)]. The kagome layers are trimerized; i.e., the bond lengths 3.249(1) and 3.065(1) Å differ for triangles with and without interconnecting trigonal sites. In $YBaCo_3FeO_7$, the smaller trivalent ion Fe^{3+} shows a preference for the trigonal site with 82(2)% occupancy, while 94(1)% of the kagome sites are occupied by Co^{2+} as determined from Mössbauer data [14]. The partial mixing seems to play a role to stabilize the high symmetry of the hexagonal lattice. The crystal field splitting in the tetrahedral oxygen environment leads to isotropic high spin states, $S = 3/2$ of Co^{2+} and $S = 5/2$ of Fe^{3+}. Indirect evidence for quenched orbital momentum with $S = 1.56(15)$ for Co^{2+} can be inferred from the site occupancies [15] and the ratio 1.25 of magnetic moments [16] for kagome and trigonal sites in the magnetically ordered swedenborgite $CaBaCo_2Fe_2O_7$.

Both magnetic ions have three t_2 electrons with similar exchange for Co-Co, Fe-Fe, and Co-Fe mediated by the superexchange paths via oxygen ions. The exchange depends on the specific material and differs for couplings in the kagome lattice J_{in} and the out-of-plane coupling J_{out} between kagome and trigonal spins. The antiferromagnetic

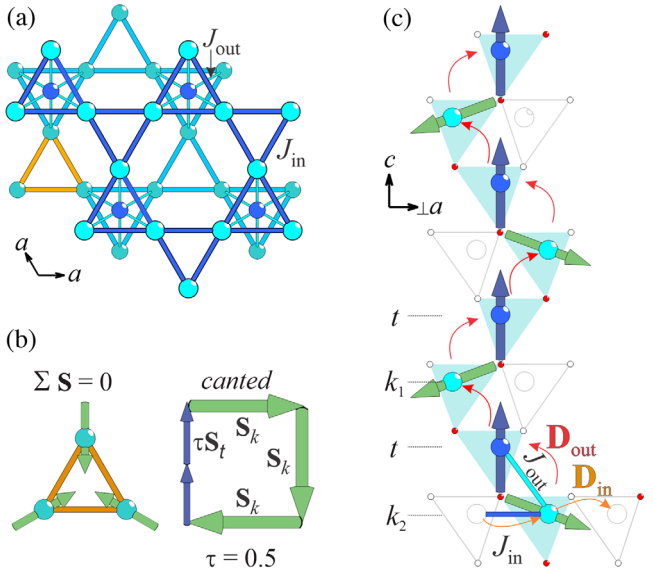

FIG. 1. Swedenborgite structure and exchange. (a) Unit cell of two trimerized kagome (k) layers (light and dark cyan) interconnected by trigonal (t) sites (blue) with nearest neighbor AFM superexchange J_{in} in the k planes and J_{out} out of plane to t sites. (b) Minimizing the configurational energy yields two sum rules, (i) implying 120° configurations of spins $\mathbf{S}_k$ on the k triangle between columns with t sites and (ii) canted configurations of spins $\mathbf{S}_k$ and $\mathbf{S}_t$ on the building unit of the columns, a k triangle capped above and below with a t site, depending on the ratio $\tau = J_{out}/J_{in}$. Spins $\mathbf{S}_t$ within each column tend to align parallel. The case $\tau = 0.5$ is proposed for $YBaCo_3FeO_7$ [14]. (c) View of the spin columns including t sites (plane ⊥ to a). All magnetic sites are tetrahedrally coordinated by oxygen, which creates antisymmetric Dzyaloshinskii-Moriya (DM) exchange on all AFM exchange paths, denoted by $\mathbf{D}_{out}$ and $\mathbf{D}_{in}$, coupling the spin space to the hexagonal lattice anisotropy. The $\mathbf{D}_{out}$ vectors, parallel to the ab plane, connect a t site with three k neighbors and select the seed for a cycloidal structure of threefold symmetry. The in-plane vectors $\mathbf{D}_{in}$ between k sites enable the further spreading of the cycloid in the kagome planes.

(AFM) interactions in such a layered kagome system are highly frustrated. The analysis of neutron scattering from a $YBaCo_4O_7$ single crystal concluded that the out-of-plane coupling J_{out} induces quasiferro-type correlations along the columns via the trigonal sites, however, it does not lift the two-dimensional frustration in the kagome planes [17]. The degeneracies can be captured by two sum rules, displayed in Figs. 1(a) and 1(b). This spin liquid orders upon an intervening structural transition breaking the hexagonal symmetry and lifting part of the frustration.

Magnetic long-range order with partial remaining disorder has been observed in $CaBaCo_2Fe_2O_7$, still preserving the hexagonal symmetry [15,16]. A completely different magnetic behavior is observed in the closely related, hexagonal $YBaCo_3FeO_7$: according to neutron scattering data of a polycrystalline sample, a spin liquid with pronounced short-range order is observed down to low temperatures, $T = 1.2$ K, despite the very strong AFM

superexchange and a Curie-Weiss temperature lower than −1000 K [14]. The observed diffuse magnetic scattering was modeled in Monte Carlo simulations applying a Heisenberg Hamiltonian with AFM nearest neighbor exchanges for $\tau = J_{out}/J_{in} \approx 0.5$ [14]. According to Monte Carlo simulations considering the simplified, but generic J_{in}-J_{out} model [16,18,19], the system is centered in a broad region of spin liquid states and should exhibit largely canted spin configurations; see Fig. 1(b). Furthermore, a symmetry analysis predicts the possibility for a chiral spin liquid phase [20]. As the inversion symmetry is broken by the neighboring oxygen mediating all superexchange paths, antisymmetric Dzyaloshinskii-Moriya (DM) interactions come into play. Their symmetry is determined by the Moriya [21] and Keffer [22] rules; see Ref. [16]. Both the frustration of J_{in} and J_{out} as well as the alternating DM interactions favor the replication of correlations along the c direction. DM terms are typically small compared to the AFM exchange with minor effect in modifying the spin canting angles. However, their qualitative influence is strong by coupling the spin space to the lattice anisotropy and giving preference for a specific cycloidal chirality of threefold symmetry in the manifold of degenerate spin configurations of this highly frustrated system.

II. SAMPLE AND EXPERIMENTAL SETUP

The here investigated single crystal was grown by the same floating zone image furnace technique described in Ref. [23]; see also Ref. [24]. The only difference was that the seed was an oriented single crystal of about 1 cm size to ensure that the wanted crystal structure axis was parallel to the growth direction; see Fig. 2.

Swedenborgites are prone to oxygen nonstoichiometry. Especially the material $YBaCo_3FeO_7$ was, at an early stage, investigated and patented as a possible oxygen storage [25] and membrane for fuel cells [26], but it was also realized that the oxygen content affects the lattice symmetry. At large oxygen surplus, the lattice is orthorhombic [27], as was also confirmed for $YBaCo_4O_{8.2}$ [28]. However, a lower than hexagonal symmetry has been reported for various swedenborgite compounds synthesized in air with smaller deviations from ideal oxygen stoichiometry. For the present case, the single crystal of $YBaCo_3FeO_7$ was grown from a melt under highly reducing atmosphere without any crucible present (zone melting under pure Ar in a mirror furnace). Under these synthesis conditions, it is clear that the material, used in our investigation, is oxygen stoichiometric (O_7). Further, the hexagonal symmetry on a minor piece of our sample ($P6_3mc$, no. 186) [24] was confirmed by a single crystal x-ray diffraction experiment.

FIG. 2. Single crystal $YBaCo_3FeO_7$, cylindrical axis $\|c$.

The diffuse scattering with polarization analysis has been measured at the DNS instrument at the Maier-Leibnitz Zentrum in Munich. The single crystal was mounted with its c axis perpendicular to the scattering plane in the DNS instrument. The lattice parameters of the hexagonal plane are $a = b = 6.3$ Å. Measurements were performed with a neutron wavelength of 4.11 Å in stepwise rotations of 1° around the c axis by taking data in 24 ^{3}He detectors with two detector bank positions. The data cover a section of 180° in the ($hk0$) plane with a grid of 1° and 2.5° in sample rotation and detector angle, respectively. For each sample position, measurements in spin-flip mode were taken with polarization and polarization reversal along the direction of $\mathbf{Q}$ for the center of the multidetector. Each single measurement took 25 s yielding typically in the order of 1000 counts near the diffuse peaks. The data were calibrated with a vanadium reference, for detection efficiency, and with a nonmagnetic $Ni_{0.89}Cr_{0.11}$ reference for ideal polarization. An intensity modulation on the order of ±10% for symmetry equivalent data was observed, due to a slightly acentric sample rotation, and was corrected for.

III. EXPERIMENTAL RESULTS

A. Methodical aspects

The present observation of a chiral spin liquid in a $YBaCo_3FeO_7$ single crystal has been made with polarized diffuse neutron diffraction, using an extension [29] of the conventional XYZ polarization analysis [30]. A common standard in polarized neutron scattering is the Cartesian coordinate system XYZ, with $X\|\mathbf{Q}$, Y in orthogonal direction, both X and Y in a horizontal scattering plane, and Z pointing in the vertical direction. Note the full magnetic scattering including chiral terms is measured in spin-flip scattering with $\mathbf{P}\|\mathbf{Q}$ (i.e., $\|X$) [31,32]. The so-called XYZ method [30] is devised for a horizontal multidetector system, where the polarization cannot be set simultaneously parallel to $\mathbf{Q}$ for the whole detector. Therefore, one considers more generally a coordinate system, which is rotated around the vertical axis Z by the angle between $\mathbf{Q}$ and $\mathbf{P}$. In the following, this coordinate system will be denoted as $X'Y'Z$. The extended XYZ method [29] includes polarization reversal, which in particular allows for the determination of the chiral part of the scattering. Furthermore, instead of an arbitrary orientation of $X'Y'$ in the plane, X' is specifically chosen parallel to $\mathbf{Q}$ for the center of the detector, which minimizes necessary corrections in the analysis; see Ref. [29].

B. Observation of antisymmetric diffuse magnetic scattering

At low temperatures, $T < 10$ K, the evolution of the diffuse magnetic scattering appears to be near saturation

and persists even at very low temperature 30 mK. No magnetic long-range order is observed. The most complete dataset of the ($hk0$) scattering plane, taken at $T = 4$ K, is presented in Fig. 3. In the notation of Ref. [29], $I_{x'\bar{x}'}$ and $I_{\bar{x}'x'}$ are the spin-flip scattering with the polarization set parallel and antiparallel to X', respectively. The diffuse magnetic scattering is broadly distributed along the hexagonal Brillouin zone boundary (BZ), which is noteworthy and a sign of strong frustration. Comparing equivalent M points of the hexagonal BZ of the kagome lattice, one observes an intensity modulation of a larger k vector, which relates to the nearest spacings between trigonal to kagome sites. In the zone center, relics of nuclear Bragg scattering still appear with high, yet nonperfect polarization. The most important feature, however, is the antisymmetry of the diffuse scattering with respect to the mirror symmetry, which reverses with the direction of **P**, compare top and bottom part of Fig. 3, and reveals the chiral properties of the system.

C. Separation of chiral scattering

A separation of the chiral part in the magnetic scattering is possible by symmetry. The symmetric part can be related to the magnetic scattering from scalar products of magnetic moments, while the antisymmetric part relates to chiral scattering from vector products of magnetic moments. Reversal of polarization **P** reverses the antisymmetry of the pattern; see Fig. 3. Accordingly, the chiral intensity is obtained by taking the difference of the two datasets,

$$\sigma^{\text{chiral}}_{\mathbf{Q}} = I_{x\bar{x}} - I_{\bar{x}x} = i\mathbf{P}\cdot(\mathbf{M}^{\perp}_{-\mathbf{Q}} \times \mathbf{M}^{\perp}_{\mathbf{Q}}), \tag{1}$$

where $\mathbf{M}^{\perp}_{\mathbf{Q}}$ represents the magnetic scattering amplitude, which includes only components perpendicular to **Q** due to the dipolar type of interaction. Therefore, the cross-product $\mathbf{M}^{\perp}_{-\mathbf{Q}} \times \mathbf{M}^{\perp}_{\mathbf{Q}}$ points parallel to **Q** and appears in projection of the polarization **P**. The chiral intensity $\sigma^{\text{chiral}}_{\mathbf{Q}}$ is corrected by the polarization quality of the instrument (typically > 0.9) and by taking into account the cosine of the enclosed angle between **P** and the actual **Q** (by which we change now from the coordinate system $X'Y'Z$ to XYZ). In order to obtain the normalized chiral scattering function $S^{yz}_{\mathbf{Q}}$, the average magnetic form factor of Co and Fe is included within dipole approximation, residuals of nuclear Bragg intensities have been removed, and finally, intensities are calibrated for a classical $S = 1$ spin model. The proper scaling implies absolute cross sections as obtained from an analysis of the total magnetic scattering, which will

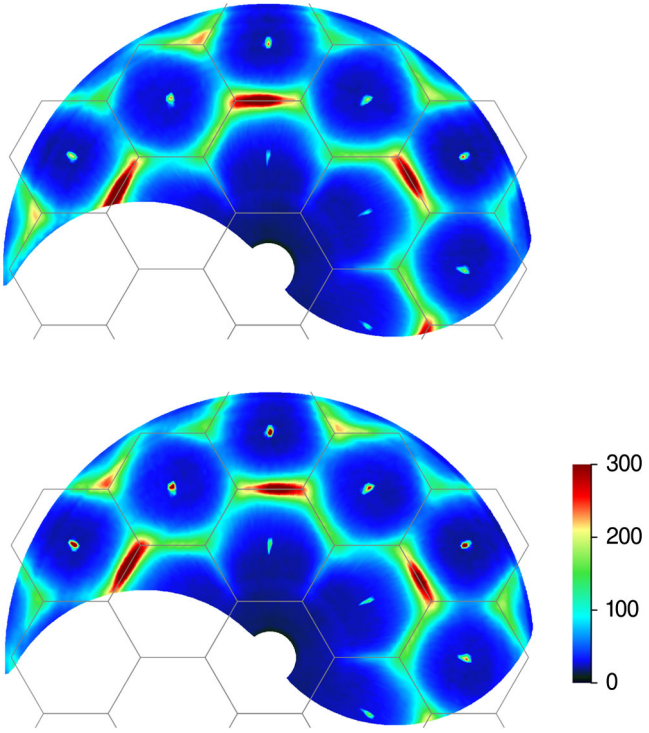

FIG. 3. Diffuse magnetic scattering of the $YBaCo_3FeO_7$ single crystal $T = 4$ K, in the ($hk0$) scattering plane. Top: $I_{x'\bar{x}'}$, spin-flip scattering with $\mathbf{P}\|X'$; bottom: $I_{\bar{x}'x'}$, polarization reversal $\mathbf{P}\| - X'$. Note the deviation from the mirror symmetry. This antisymmetric part reverses with the direction of **P** and is a direct sign of the underlying cycloidal chirality. (Intensities are given in neutron counts/s, while measuring all points for 25 s. Number of independent data points is 8640. The hexagonal Brillouin zone of the nuclear unit cell is shown in gray.)

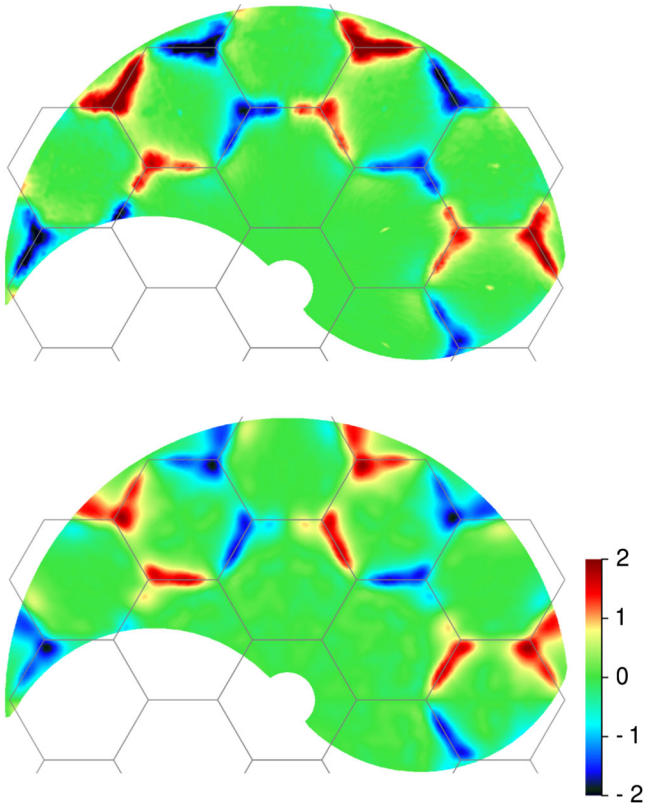

FIG. 4. Top: normalized observed chiral scattering $S^{yz}_{\mathbf{Q}}$. Bottom: modeled chiral scattering based on cycloidal chiral correlations obtained by Fourier analysis.

be given in a forthcoming paper. The observed chiral scattering function $S^{yz}_{\mathbf{Q}}$, shown in Fig. 4 (top), confirms the postulated chiral spin liquid state in $YBaCo_3FeO_7$ [20].

D. Fourier analysis in terms of chiral correlation functions

In the following new approach, we aim for a real-space interpretation of the diffuse chiral scattering by establishing the Fourier representation in terms of chiral correlation functions, which requires a rigorous decomposition of the polarized scattering tensor into an orthonormal basis. The application requires data of sufficient high quality and extent in reciprocal space.

In the van Hove interpretation of the scattering, $S^{yz}_{\mathbf{Q}}$ is the Fourier transform of the chiral spin correlation function $G^{yz}_{\mathbf{r}} = \langle S^y(0)S^z(\mathbf{r})\rangle$. Recall that terms with S^x ($\|\mathbf{Q}$) are not seen via the dipolar interaction with neutrons. Polarized neutron scattering from single crystals can probe directly the expectation value for the vector chirality between spins at distant sites:

$$\mathbf{C} = \mathbf{S}_{\mathbf{R}} \times \mathbf{S}'_{\mathbf{R}'}. \tag{2}$$

We can distinguish $G^{yz}_{\mathbf{r}}$ and thus $S^{yz}_{\mathbf{Q}}$ for three different propagations, in x, y, and z directions:

$$\begin{aligned} S^{yz}_{\mathbf{Q}} &= i\mathbf{P}\cdot\mathbf{C}(\mathbf{Q}) \\ &= \sum_{\mathbf{r}} \mathbf{e}_{\mathbf{Q}} \cdot \begin{pmatrix} G^{yz}_{x,\mathbf{r}}\ \mathbf{e}_{\mathbf{r}_\parallel} \\ G^{yz}_{y,\mathbf{r}}\ \mathbf{e}_{\mathbf{r}^y_\perp} \\ G^{yz}_{z,\mathbf{r}}\ \mathbf{e}_{\mathbf{r}^z_\perp} \end{pmatrix} \sin(\mathbf{Q}\cdot\mathbf{r}), \\ &= \sum_{\mathbf{r}} \begin{pmatrix} G^{yz}_{x,\mathbf{r}}\ \mathbf{e}_{\mathbf{Q}}\cdot\mathbf{e}_{\mathbf{r}} \\ G^{yz}_{y,\mathbf{r}}\ \|\mathbf{e}_{\mathbf{Q}}\times\mathbf{e}_{\mathbf{r}}\| \\ 0 \end{pmatrix} \sin(\mathbf{Q}\cdot\mathbf{r}). \end{aligned} \tag{3}$$

The components of G are scalar coefficients for applying a Fourier analysis associated with their unit vectors of propagation. The first term describes a helix, its unit propagation vector $\mathbf{e}_{\mathbf{r}_\parallel}$ is parallel to $\mathbf{C}$, and $\mathbf{C}$ is seen in projection to the scattering unit vector $\mathbf{e}_{\mathbf{Q}}$. The second term describes a cycloid with a unit propagation vector $\mathbf{e}_{\mathbf{r}^y_\perp}$ perpendicular to $\mathbf{C}$. The contribution to scattering is the projection of $\mathbf{C}$ to $\mathbf{e}_{\mathbf{Q}}$, which is given by the projection of the in-plane perpendicular direction to $\mathbf{e}_{\mathbf{Q}}$. The third term describes a cycloid propagating along z perpendicular to $\mathbf{C}$. Of course, propagations along z cannot be seen in the scattering plane ($hk0$) and require sufficient data along l and with components of $\mathbf{P}$ along [001]. The given basis set is complete with respect to a Fourier analysis of the measured data. In principle, these terms describe also any combination of the pure chiral modes, constituting, for example, of a tilted helix by a combination of cycloidal and helical modes. Furthermore, a cycloid propagating with both spin components in the ab plane is not visible in the ($hk0$) scattering plane, because one component S^x is parallel to $\mathbf{Q}$. We note that chiral scattering is a result of interference without self-term and its intensity average is zero. The chiral scattering function $S^{yz}_{\mathbf{Q}}$ represents a fully antisymmetric scattering tensor, which can be identified as the sin-Fourier transforms of the components of helical and cycloidal correlation functions. These components can be distinguished by symmetry with respect to their propagation vectors, causing antisymmetry parallel to $\mathbf{Q}$ in the case of a helix, and antisymmetry perpendicular to $\mathbf{Q}$ in the case of a cycloid. The observed specific antisymmetry of $S^{yz}_{\mathbf{Q}}$ perpendicular to the scattering vector Q agrees with the threefold lattice symmetry. Hence, three cycloidal modes contribute equally in generating a cylindrical cycloidal pattern.

Fourier analysis according to Eq. (3) yields the chiral pair correlation G^{yz}_r, displayed in Fig. 5, and it is possible to probe both cycloidal and helical correlations. The measured $S^{yz}_{\mathbf{Q}}$ is essentially described by only cycloidal correlations, given by the coefficients $G^{yz}_{y,r}$ in Eq. (3), while helical terms related to $G^{yz}_{x,r}$ are found to be negligible. Figure 4 shows a comparison of the observed and calculated chiral scattering (top and bottom, respectively) as obtained from the Fourier coefficients of the cycloidal correlations. It is obvious that the model captures convincingly the characteristic features of the experimental data. Technically, the Fourier analysis is performed within a linear least square procedure as it has been applied to the diffuse scattering of binary alloys [33]. We can actually distinguish correlations between spins at trigonal and kagome sites from those of spins at separations of the kagome sublattice, shown in blue and red, respectively. The correlations that involve the trigonal site are significantly larger in amplitude than correlations among

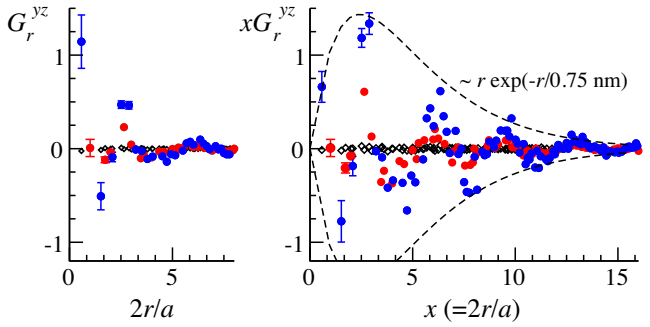

FIG. 5. Chiral spin correlations. Left: chiral correlation function G^{yz}_r as obtained by Fourier analysis. Cycloidal correlations $G^{yz}_{y,\mathbf{r}}$ of $3f$ symmetry including the triangular site (blue) are dominant with respect to cycloidal correlations between only kagome sites (red). Helical correlations $G^{yz}_{x,\mathbf{r}}$ are negligible (black). Right: G^{yz}_r scaled with distance to show the extent of observable correlations and compared to an asymptotically exponential decaying envelope.

the kagome spins. This concurs with the expectation that the DM interaction between neighboring trigonal and kagome spins is the origin of the cycloidal chirality and further agrees with the threefold symmetry of $S^{yz}_{\mathbf{Q}}$ in Fig. 4. The true range of observable chiral correlations is revealed at larger distances by scaling G^{yz}_r with r as shown in the right-hand part of Fig. 5.

There are significant cycloidal chiral correlations with oscillating amplitudes revealing a radial wavelike pattern, with a relatively large wavelength of about 1 nm and five notable periods.

A large number of lattice vectors has been used in the Fourier analysis, distinguishing 100 parameters for kagome distances and further 100 parameters for distances involving the t sites. It was necessary to limit the analysis to the ideal kagome lattice rather than for the actual trimerized structure. We assume that the overall results will only weakly depend on details such as trimerization. Because of the limited resolution, i.e., the large wavelength of the neutron beam, the data are not sufficient to discriminate reliably between the splitting of the kagome bond lengths. This limitation is probably causing the minor systematic discrepancies between data and modeling. The analysis is stable for the large tail of correlations with small errors only (below symbol size). The error bars in Fig. 5 have been estimated by including systematic variations of model size. However, these variations also show that the first two correlation parameters for nearest and next-nearest neighbors are indeed more uncertain due to the limited Q range of the experiment. The chiral correlations show an asymptotic exponential decay length of approximately 0.75 nm, see Fig. 5, comparable to the period length. The shown experimental data are limited to the (hk0) scattering plane and describe the correlations perpendicular to the c axis. Further experiments did not show any diffuse chiral modulations in c direction. The total diffuse magnetic scattering is rather concentrated in the basal scattering planes. The out-of-plane peak width is small and indicates a decay length of approximately 1.3 nm. Therefore, we have to assume that the planar spin correlations simply replicate in c direction, yielding a cylindrical shape of the threefold cycloid. This pattern is exactly expected from the underlying interactions; see Fig. 1. The sum rule for the AFM superexchange yields ferro-type correlations for the coupling interlayers of trigonal sites.

E. First discussion of the experimental results

The observed cylindrical symmetry and anisotropy of the cycloidal correlations is consistent with the hexagonal crystal structure and can be traced back from the antisymmetric Dzyaloshinskii-Moriya interactions appearing with threefold symmetry around the trigonal sites [16]. Typically, such DM terms are relatively weak, and thus the strong chiral correlations may be a surprise. An explanation can be found in the strong geometric frustration of the AFM exchange. As proposed earlier [14], for a ratio $\tau = 0.5$, local spin configurations are fully canted, still with remaining degrees of freedom in 3D space. It is fair to assume that the DM interactions are, as typical, relatively weak. However, when they come into play, their effect can be strong, determining a definite handiness and further coupling the spatial polar anisotropy to the spin space. The proposed scenario is that a cylindrical cycloid starts to grow around the trigonal sites in a chiral lumplike pattern. The extent of the chiral correlations signifies further the role of the in-plane DM exchange between k sites in spreading the cycloidal pattern in the kagome plane. For visualizing such a chiral lump, in first approximation, one may consider the generating DM interactions, see Fig. 1, and the chiral correlation function itself by choosing a trigonal site as the origin with its proper polar axis and anisotropy; see Fig. 6. The local spin configurations are consistent with the DM exchange and the strong AFM exchange, local and global sums of spins equal to zero; the core shows a nearly spin tetrahedral configuration, and second and third neighbor spins are almost antiparallel oriented (Fig. 6). The extent of this lump pattern is large but appears exaggerated with the chosen scaling, which suggests an interwoven assembly of such chiral lumps.

Apparently, the chiral seeds do not further grow into a coherently ordered state. It has been observed that the spin dynamics is slowing down near 40 K [14]. A study of a similar swedenborgite compound led to the speculation of a glass transition due to bond disorder [34]. The present results shed new light on the so far hidden and emerging chirality, which severely reduces the configuration space of this frustrated spin system and consequently its dynamics. The temperature scale may serve for a first estimate of the DM exchange. On real time scales, the system is not frozen since the diffuse intensity and thereby the chiral

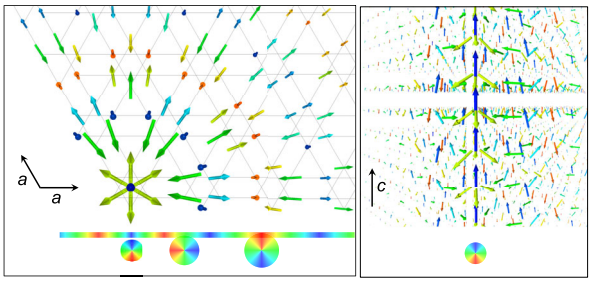

FIG. 6. Chiral lump pattern as obtained in first approximation from the chiral correlation function: left, top view projection; right, perspective side view. Chiral spin correlations are mapped around a trigonal site, which is considered as the origin of a magnetic lump. Neighboring spins are scaled with distance from the center for emphasis only analog to Fig. 4 (right). The color wheel illustrates the spin angle and phase of the cylindrical cycloid. Spins show upward (blue) in the center of the lump, which reflects the polar anisotropy. This choice is arbitrary with respect to the degeneracy of spin inversion.

correlations further evolve upon cooling reaching a saturation level below 10 K. Still the lack of order at very low temperatures appears to be a miracle that is considered below within the classical theory of magnetic ordering.

IV. THEORETICAL CONCEPT FOR AN INHOMOGENEOUS CHIRAL GROUND STATE OF FINITE CORRELATION LENGTH

In search of a theoretical concept, the origin of the observed specific chirality has to be found in the role of the present antisymmetric DM exchange. In a second view, the lack of order in this strongly interacting spin system imposes the more fundamental challenge. As we lay out, this can be explained within the standard theory of magnetic ordering and is valid even for a clean magnetic system, i.e., in the absence of quenched disorder.

From a fundamental perspective, the unavoidable DM exchange in this three-dimensional noncentrosymmetric magnetic system is known and able to prevent a classical ordering phase transition at finite temperature. Hence, anomalous cooperative magnetism is the expected behavior. This is described by the violation of the Lifshitz criterion in the phenomenological Landau theory [35]. Using minimal assumptions about this spin systems, namely, the existence of several nearly degenerate ordering modes, which is the rule in a geometrically frustrated multisublattice antiferromagnets, and the existence of this chiral antisymmetric exchange, the generic properties of this magnetic system do not allow a standard classical phase transition into a long-range ordered state. Instead, the frustration caused by the chiral DM interaction is able to generate localized entities which may condense into mesophases that may be ordered or remain disordered. This is a general mechanism for chiral helimagnets with DM interaction [36,37]. Eventual condensation of such entities then is driven by different weaker forces which still may remain frustrated at larger scales. A prominent example for the condensation of spins into an inhomogeneous magnetic state is known for chiral helimagnets, the assembling of skyrmions into dense-packed lattices [38]. Extending this theory to describe the coupling of several ordering modes via the DM interaction, the analysis demonstrates the anomalous magnetic ordering and the creation of a lumplike pattern of individual zero-dimensional entities as a generic behavior that can occur in a large class of acentric magnetic systems. We use the standard phenomenological free-energy expansion according to Landau theory [35], which describes the tendency of the spin system to develop a long-range ordered state. For the considered class of crystalline three-dimensional materials, the existence of the so-called Lifshitz invariants then is a sufficient criterion to decide whether an ordinary phase transition into a long-range ordered state is impossible. Thus, only symmetry considerations are necessary to decide whether this criterion is violated.

A. Basic mechanism

The physical mechanism underlying these free-energy contributions in a spin system, however, is given by the antisymmetric Dzyaloshinskii-Moriya exchange. The second vital assumption is the existence of a larger number of components of the relevant order parameters. These could be given by energetically almost degenerate magnetic sublattices or other spin patterns with internal degrees of freedom in models that describe a large (isotropic) exchange coupled spin system and its tendency for cooperative ordering. The primary modes of a possible magnetic order, thus, are given by the so-called exchange approximation which defines a set of possible order parameters. In the swedenborgite-lattice magnetic systems, the geometrically frustrated antiferromagnetism allows for a multitude of such coexisting primary modes. Under the influence of the antisymmetric exchange, owing to the polar lattice structure, these modes are both twisted into handed spirals, but also mutually coupled. The Landau-Ginzburg expansion allows us to formulate general free-energy densities for such systems [39]. The form of the resulting free energies with many order-parameter components, however, is general, as it depends essentially only on the broken spatial parity in noncentrosymmetric crystal classes. Therefore, it is not required to identify the exact nature of the primary modes. For simplicity, we refer to them as sublattice spins. The simplest version of such models is given by a noncentrosymmetric magnetic crystal with sublattices having two different primary order parameters which are energetically degenerate. For simplicity, we may assume that they are three-component axial vectors describing, e.g., the orientation of the staggered Néel vector, φ_1 and φ_2 with components written as $\varphi_{i\alpha}$. Using Landau theory to describe these two coupled primary modes, we write a phenomenological continuum theory for the ordered spin structure including spatial gradient terms $\partial_\gamma \varphi_{i\alpha}$ order-parameter components. For certain classes of noncentrosymmetric magnets, with the appearance of antisymmetric exchange $\mathbf{D}$, we then see that the Landau theory allows for Lifshitz invariants, terms linear in one spatial gradient of the order parameters φ_i and antisymmetric:

$$D^{(\gamma)}_{\alpha\beta}(\varphi_{i\alpha}\partial_\gamma\varphi_{i\beta} - \varphi_{i\beta}\partial_\gamma\varphi_{i\alpha}), \quad i = 1, 2. \tag{4}$$

The Landau-Ginzburg function for each of the modes is given by

$$\begin{aligned} w_i = {} & A_i(\nabla\varphi_i)^2 + D^{(\gamma)}_{\alpha\beta}(\varphi_{i\alpha}\partial_\gamma\varphi_{i\beta} - \varphi_{i\beta}\partial_\gamma\varphi_{i\alpha}) \\ & + a_i(T - T_{ci})|\varphi_i|^2 + b_i(|\varphi_i)|^2)^2, \quad i = 1, 2, \end{aligned} \tag{5}$$

where the last two terms are the standard Landau expansion. Below the critical temperatures T_{ci}, this model describes a chiral spiral ground state with a modulation

length which is determined by the ratio of direct exchange and antisymmetric exchange, here given by the ratio A/D for appropriate combinations of materials coefficients A_i and $D_{\alpha\beta}^{(\gamma)}$ [36,39].

For the two different magnetic modes of the model, individually, these modulation lengths may be different. In addition, there are *Lifshitz-type* invariants that couple the different modes; e.g., for our model they look like

$$G_{\alpha\beta}^{(\gamma)}(\varphi_{1\alpha}\partial_\gamma\varphi_{2\beta} - \varphi_{2\beta}\partial_\gamma\varphi_{1\alpha}), \tag{6}$$

where the materials coefficients $G_{\alpha\beta}^{(\gamma)}$ derive from antisymmetric exchange couplings between different primary modes. Usually, such terms are irrelevant, if one of the ordering modes is a primary order parameter which orders first, and the second mode forms only under its influence. However, near a multicritical point, $T_{c1} \simeq T_{c2}$, where the different modes order simultaneously, the influence of this Lifshitz-type coupling leads to a mutual influence between the ordering modes onto the other. This means that possible ordered states have to be described in an enlarged order-parameter space spanned by $\boldsymbol{\phi} = (\varphi_1, \varphi_2)$ and internal rotation occurs because of the existence of the Lifshitz-type invariants. The competition with other coupling terms between these order-parameter components then will introduce additional length scales in the system; i.e., the Lifshitz-type invariants determine an additional modulation length for configurations where the two order parameters can alternatingly exist by an internal rotation from sector 1 to sector 2 of the enlarged order-parameter space. This basic theory then holds a set of competing lengths scales for the twisting of order parameters and the transmutation of one ordering mode into another. This encodes the generic frustration of multisublattice magnets near multicriticality and with twisting antisymmetric exchange forces. The presence of this set of different Lifshitz(-type) invariants in the free-energy expansion violates the third criterion of Landau theory, the Lifshitz criterion, in almost all cases. This means that the system cannot undergo a conventional continuous phase transition, where the ordering modes develop into a homogeneous state of order.

The frustrating effect of the DM interactions in multisublattice magnetic systems with coexisting ordering modes can be captured in a continuum with a frozen gauge background, as seen by rewriting the gradient part of the free energy,

$$W = A(\nabla\boldsymbol{\phi})^2 + \Delta_{\alpha\beta}^{(\gamma)}(\boldsymbol{\phi}_{i\alpha}\partial_\gamma\boldsymbol{\phi}_{i\beta} - \boldsymbol{\phi}_{i\beta}\partial_\gamma\boldsymbol{\phi}_{i\alpha}), \tag{7}$$

and, by closing the square on the gradient terms and rescaling, this expression can be rewritten in a form

$$W = [(\partial_\gamma + d_{\beta\alpha}^{(\gamma)})\boldsymbol{\phi}_\alpha]^2 + \text{anisotropic terms}, \tag{8}$$

with new sets of materials coefficients A, Δ, and d. This is an expression akin to minimal coupling with a gauge field, if the set of $d_{\beta\alpha}^{(\gamma)}$ parameters would be dynamical degrees of freedom. Phenomenological free energies with frozen gauge background of this type can be called Dzyaloshinskii models as Dzyaloshinskii developed such a continuum theory in the context of chiral magnetism in Ref. [39]. For our model these expressions are fixed or frozen. Setting the expression within square brackets in Eq. (8) to zero,

$$(\partial_\gamma + d_{\beta\alpha}^{(\gamma)})\boldsymbol{\phi}_\alpha = 0, \tag{9}$$

yields the linear Bogomol'nyi equations of the model that approximate the multiply twisted core region of lumps described by this continuum theory, if gradient terms are allowed for the three Cartesian spatial directions $\gamma = x, y, z$.

B. Primitive model for swedenborgite-lattice spin systems

A primitive model for classical order-parameter modes of a material like $YBaCo_3FeO_7$ may be constructed from a set of sublattices, which describes a spin pattern and respects the symmetries of possible couplings. The simplest approach combines the spins on different sites into spin patterns, which are described by a set of axial vectors $\mathbf{l}$, $\mathbf{m}$, $\mathbf{n}$, etc. The geometrical frustration inherent in the lattice structure will naturally lead to the (multicritical) degeneracy for several of these primary modes. Thus, a statistical field theory for these spin systems may be represented by a large set of these axial vector fields. For the crystal class C_{6v} (or $6mm$) of the swedenborgite lattice, the Lifshitz invariants for coupled axial vectors, represented as continua of fields, have the form [36]

$$D_l(l_x\partial_x l_z - l_z\partial_x l_x + l_y\partial_y l_z - l_z\partial_y l_y)\ldots, \tag{10}$$

and Lifshitz-type invariants with the form

$$g_{lm}(l_x\partial_x m_z - m_z\partial_x l_x + l_y\partial_y m_z - m_z\partial_y l_y)\ldots. \tag{11}$$

These terms describe the cycloidal rotation of the spin vectors in any direction in the basal plane, perpendicular to the c axes (which is taken parallel to the z axis of the Cartesian system). However, in the polar crystal class, there are additional Lifshitz-type invariants along the c axis of the form

$$f_{lm}(l_x\partial_z m_x - m_x\partial_z l_x). \tag{12}$$

These terms lead to a modulation in c direction in the form of the discussed internal rotations of order-parameter components around each other. The gradient part of

the Dzyaloshinskii model for swedenborgite lattices, i.e., Eq. (7) with the specific Lifshitz(-type) invariants Eqs. (10)–(12), thus describes spin structures with cycloidal spirals propagating in the basal plane and contains additional frustrating terms leading to modulations between ordering modes also in the c-axis direction. This shape and internal structure of zero-dimensional lumps as extended solitonic objects can be recognized from this Dyzaloshinskii model [36,37]. The cores of these lumps are given by the corresponding Bogomol'nyi equations (9) and must display cycloidal twist radially in all directions perpendicular to the c axis, while it also has a limited extension in the c-axis direction because of the Lifshitz-type invariants (12). As in the case of skyrmions in chiral helimagnets [38], the free-energy density in the cores of these lumps is reduced compared to a single spiral, by activating several Lifshitz terms. This stabilizes these static solitonic objects and generates inhomogeneous ground states upon condensation of these lumps into a mesophase.

C. Topology and geometry of lumpy textures

Depending on the number of relevant order-parameter components $n > 3$ in three-dimensional space, the lumps will retain a set of degrees of freedom in the ideal case where the order-parameter manifold has no anisotropies and is described by a sphere $\mathcal{S}^{n-1}$. Therefore, the lumps are topologically unstable and cannot be construed as skyrmions. As usual, the textures are given by maps from the real space occupied by an infinite crystal, $\mathcal{E}^3 \cup \{\infty\} = \mathcal{S}^3$ into the manifold M encoding the order-parameter space which encodes the multisublattice spin configurations. Locally, the space can be viewed as a piece of a sphere $\mathcal{S}^{n-1}$. The extra directions in order-parameter space which describe the facility to unwind solitonic lumps also entails the possibility to rotate lumps internally without changing their energy. Therefore, the dynamics of the spin system at finite temperatures even in a condensed mesophase given by a space-filling arrangement of lumps may retain the ability to support localized fluctuations with very low energy, i.e., gapless localized modes hitched on the cores of the lumps. This suggests a possibility to form partially ordered spin arrangements, which display residual fluctuations. Therefore, Dzyaloshinskii models of type Eq. (7) are not expected to yield a conventional phase transition, but they can display a successive freezing of the spins possibly with a relatively sharp crossover from a high-temperature paramagnetic state into a lumpy condensate. This physical picture suggests that the frustration by the frozen gauge background may preserve ultimately an amorphous ground state. Such a state is expected to display a heterogeneous lumpy appearance, which is almost static. Unless these lumps themselves order into crystalline latticelike arrays, there will not arise a true long-range ordered state. Finally, a heterogeneous dynamics of low-lying excitations, in particular localized modes, will retain a certain residual dynamic in this state. Based on this picture, we may conjecture that Dzyaloshinskii models for chiral frustrated spin systems with a coexisting larger number of primary ordering modes can display amorphous ground states without any need for quenched disorder.

This picture is supported by the fact that generic continuum fields with frozen gauge background do not have any finite-temperature phase transition and avoid the ordering into a homogeneous state in the limit $n \to \infty$ [40]. It is noteworthy that such models have been used to rationalize the behavior of structural glasses and supercooled liquids. However, generically we believe that structural glasses are only metastable or even instable frozen states while the true ground state is a crystal. Here, we may argue that the frozen gauge background acting on spin systems precludes the appearance of a conventional long-range order of crystalline type.

The argument for a disordered ground state in such Dzyaloshinskii models with a frozen gauge background can be sharpened by their extension into fully fledged gauge theories and use of the Elitzur theorem [41]; see also Ref. [42]. The gauge freedom consists in an appropriate rotation of the field ϕ, which is compensated by a corresponding redefinition of the gauge fields d,

$$\begin{aligned} \phi' &= R(\mathbf{r})\phi, \\ d'_{\beta\alpha} &= g(R(\mathbf{r}))d_{\beta\alpha}, \end{aligned} \tag{13}$$

where R is a rotation matrix acting on the field ϕ and $g(R(\mathbf{r}))$ the corresponding transformation of the gauge potential, which may not be uniquely defined. A physical configuration of the spin structure is described by fixing this gauge, but this can be achieved in multiple ways. For example, a twisted configuration of the fields can be represented by a constant unidirectional effective field, $\phi' = \text{const}$, through rotating the reference frame of these gauge potentials into the local direction of ϕ, whence the effective gauge potential Eq. (13) becomes a correspondingly varying function in space, $d'_{\beta\alpha}(\mathbf{r})$. However, for ideal field configurations close to the free-energy minimum of the original model, this transformation may be used to remove the gauge potential and achieve an effective description with $d'_{\beta\alpha} \equiv = 0$. For one-dimensional spirals, this procedure is always possible; for structures twisted in several spatial directions, the corresponding simplification is achievable only locally. The conceptually related case of a spatially varying gauge background has been discussed by Hertz in a gauge-field model for spin glasses [43] with a Heisenberg-like spin structure. In the case of spin glasses, the original ungauged model has a spatially varying gauge background which describes the quenched disorder.

However, as constant frozen gauge background can host localized twisted lumps, which realize a local minimum of the free energy, there exist infinitely many different ways to fix the gauge potentials and all of them describe states close

to the free-energy minimum. If one assumes this statement to be valid, then the ordering of Dzyaloshinskii models described by Eq. (7) requires a fixing of the various possible gauge potentials. This is impossible, as the Elitzur theorem stipulates that a spontaneous local breaking of the gauge freedom cannot occur. Therefore, the multidimensional Dzyaloshinskii models may represent a type of statistical field theories which do not allow a conventional ordered ground state that could be realized by a spontaneous generation of an ordered homogeneous state. Rigorously, this has been shown for the $n \to \infty$ of our model [40]. Hence, we suggest that the frustration by the frozen gauge background similarly should be able to suppress or avoid any conventional ordering in multicritical systems with a large number or order-parameter components, too. Multisublattice spin systems with chiral DM interactions can display this type of behavior. Hence, we consider them as candidates for amorphous classical ground states. A rigorous proof of our conjecture requires a proof that assemblies of localized lumps may yield (i) a space-filling ground state with lowest possible energy and (ii) that this assembly still is frustrated again at longer scales and still cannot order into latticelike arrays. It also is an open problem whether other exotic types of ordering with unconventional transitions may occur in such models upon lowering the temperature, like in spin glasses [44].

A successive freezing of the spin systems in materials described by Dzyaloshinskii models may also encounter topological constraints that obstruct long-range order, because particular excited or defected configurations are necessarily present in order to mediate between different ideal ordered spin configurations in localized lumps that can coexist. In the case of the chirally twisted spin configurations, these are minima of the phenomenological free energy. The excitations mediating between these minima are saddle-point configurations of the continuous fields, which have been described in theory for elementary particles as sphalerons [45]. These hypothetical elementary particles are extended objects derived from quantization of instable or metastable configurations of classical continuous fields. Eventually, the existence of these sphaleron configurations is necessary, owing to the topology of possible field configurations [46]. The geometrical arrangement of the various spin textures, i.e., the maps $(\mathcal{S}^3 \infty M)$, may have topologically nontrivial properties. If the space of these maps contains topologically noncontractible loops or spheres, the existence of metastable sphalerons as excitations of the ground state may become necessary [47]; see also the discussion in Ref. [46]. This mechanism for topological obstruction is particularly relevant, when the ideal case of a target manifold $M = \mathcal{S}^{n-1}$, which displays the $\mathrm{SO}(n)$ rotation symmetry, is abandoned and the M decomposes into several disjoint subsets or submanifolds. In practical terms, this means that the freezing in of a lumpy texture may yield a metastable configuration of a spin system which is unable to achieve ordering as defects exist between the free-energy minima that cannot be healed owing to this topological protection.

D. Fragility of the chiral amorphous state

Anisotropies strong enough to block continuous rotation of the spins will prompt the appearance of preferential directions and ultimately lead to conventional long-range order. This observation may explain the fact that some swedenborgite-type spin systems order at fairly large temperatures, while $YBaCo_3FeO_7$ has a liquidlike ground state. Some of these systems order upon preceding transitions to orthorhombic or monoclinic structures of lower symmetry, which removes part of the frustration. However, the DM exchange remains present and may stabilize local excitations.

In this substituted magnetic system, the magnetic sites are mixed but have different Heisenberg spin states. But they have essentially the same exchange. The partly mixed character of the Co and Fe sites may cancel the effects of small anisotropies, possibly arising from real exchange anisotropy, i.e., higher-order effects of the spin-orbit coupling, and any single-ion or dipolar anisotropic couplings between the spins in the effective coarse-grained continuum model. A pure spin system without this smoothened anisotropy may instead undergo a transition to a long-range order state. Essentially, the twisting influence of the DM exchange on the spin system is too weak to overcome the orientation of spins in preferred directions. In the theoretical language of the previous section, such anisotropies break gauge invariance sufficiently and invalidate any argument for disordered ground states based on the gauge freedom. At the level of the primitive model with two interacting primary modes, we may illustrate the effect of anisotropies by writing down the leading anisotropic terms for a polar system from crystal class C_{nv}, $n = 2, 3, 4, 6$; the cases $n = 2$ and $n = 6$ begin being relevant for swedenborgite-lattice magnetic systems. The first term is exchange anisotropy:

$$w_a = k_a(\partial_x \varphi_{ix})^2 + k_b(\partial_y \varphi_{iy})^2 + k_c(\partial_z \varphi_{iz})^2. \quad (14)$$

For cases $n = 3, 4, 6$ the coefficients fulfill $k_a \equiv k_b$. The next term describes the magnetocrystalline anistropy:

$$w_A = K_1(\varphi_{ix})^2 + \text{higher order terms}. \quad (15)$$

These two terms are the standard contributions for a magnetic ordering mode which dictate the direction of magnetic moments. Their combined effect also influences the orientation inhomogeneities like a magnetic wall or of the cycloidal spiral caused by the chiral DM interaction. A very large effect of the magnetocrystalline anistropy (15) will suppress the spiral state completely, and only a homogeneous order is observed. In addition to the proper magnetic anisotropies in real space, the coupled model of these modes also illustrates the anisotropy in the

order-parameter space. The standard Landau expansion for these two modes also requires quartic terms:

$$w_4 = b_i(\varphi_i \cdot \varphi_i)^2 + c(\varphi_1 \cdot \varphi_1)^2(\varphi_2 \cdot \varphi_2)^2 + \text{higher order terms.} \quad (16)$$

The materials coefficients b_1, b_2, c then favor certain orientations of the combined order parameter ϕ near the multicritial point, i.e., temperatures close to $T_{c1} \simeq T_{c2}$. Near this point, the collection of the free energy contributions Eq. (5) with the Lifshitz(-type) invariants (4), (6) the higher-order terms from Landau expansion (16), and the higher-order anisotropic terms (14), (15) describe a system which can display various conventional ordering phenomena like standard collinear Néel order, a Dzyaloshinskii-spiral ordering, i.e., one mode twisted under the influence of the DM interaction, However, the same set also describes the lumpy structure composed of the two modes, if the degeneracy of the modes is not lifted by the anisotropies and the Lifshitz(-type) invariants (4), (6) are sufficiently strong. Hence, the generic phenomenology of possible ordered magnetic states on a polar lattice structure, such as the swedenborgite lattice, comprises a vast set of possible behavior. The lumpy amorphous structure can be realized only if both anisotropies, the real-space magnetic ones, and the energetic differences encoded in the mode-coupling terms Eq. (16) are sufficiently small.

The ordering of these lumpy entities into a long-range ordered array may remain incomplete, as the frustration of the chiral couplings remains appreciable at all scales, and the condensates may appear as amorphous textures. This means that beyond a certain length scale related to the twisting of the primary ordering-modes, a long-range order is not detectable any more—and no true phase transition between the paramagnetic state, i.e., the liquidlike or gaslike fluid, and the ground state takes place. It is noteworthy that a similar idea is used to describe the atomic short-range order of structural glasses, where locally preferred clusters do not assemble into extended states [48]. Indeed, in the limit of an ordering described by infinitely many primary modes, the avoidance of true long-range order has been rigorously shown [40]. This suggests that magnetic systems can display similarly avoided long-range ordering and may prefer to remain in a disordered finite-temperature state down to lowest temperature, although they develop a correlated lumpy texture of finite range. Thus, they form an amorphous or liquidlike ground state. The ingredients for this mechanism are specific to certain structures (i) There should exist many nearly degenerate ordering modes. Geometrically frustrated antiferromagnets owing to their extensive ground-state manifold fulfill this requirement. (ii) A frustrating frozen gauge background should act on, and mutually couple, these degenerate modes in the appropriate continuum description for these ordering modes. The microscopic DM interaction in the noncentrosymmetric structure are an easily recognizable form for this mechanism, as the broken inversion symmetry alone guarantees the existence of the appropriate chiral couplings.

V. CANDIDATE MATERIALS FOR CHIRAL SPIN LIQUID GROUND STATES

The proposed classical mechanism for amorphous ground states of spin systems should exist in various other magnetic and clean crystalline materials, i.e., crystalline compounds with magnetic sublattices and in the absence of quenched disorder that could lead to a spin-glass ground state. Table I lists a few materials that can be considered as candidates for this mechanism. This table has been assembled by considering the following points. The crystallographic symmetry of the lattice is known and noncentrosymmetric in such a manner that simple ordering of magnetic spin systems should be described by Dzyaloshinskii models of type Eq. (8). Thus, Dzyaloshinskii-Moriya exchange is present and allows for Lifshitz(-type) invariants in the phenomenological free energy of possible (simple) spin ordering. Additionally, we list only materials that have already received some attention and are known to display unconventional magnetic properties, such as multiple-k spin structures, spin liquid or glassy states. Our search, therefore, does not restrict the materials classes that can be considered as candidates, as the selection criteria rely only on lattice symmetry and available experimental information. The table is not exhaustive by far. For some materials listed, the ground state is long-range ordered. In particular, for the swedenborgite-type materials, these examples are included to mark the possible contrast between systems, which do remain in a spin liquid state, and others which undergo an ordering phase transition, e.g., under the influence of sufficiently strong anisotropies. In the latter systems, the twisted chirally correlated spin textures may still be observed above the ordering transition in an intermediate state, as mesophases. These are the parent mesophases or precursor phenomena of chiral helimagnets [49,50].

A symmetrically similar cycloidal chiral spin liquid state is expected for the isomorphic compound $Y_{0.5}Ca_{0.5}BaCo_4O_7$. While studies on powder samples do not allow conclusively for distinguishing between proposed two- [51] and three-dimensional [34] spin structures, the latter case is clearly confirmed by a recent single crystal study [52]. It is common to this and the title compound that the spin dynamics is slowing down upon lowering the temperature and becomes quasistatic on the timescale of neutron scattering and neutron spin-echo spectroscopy [14,34]. $S(Q)$ evolves continuously below 50 K, where the line width is already resolution limited in neutron spin-echo spectroscopy, however, not in a diverging manner but reaching a saturating level near 10 K. The spin dynamics of $YBaCo_3FeO_7$ has further been studied by Mössbauer [14], NMR, and ESR spectroscopy [53]. The temperature dependence of the line width ΔH in high field ESR [53]

TABLE I. Frustrated spin systems with potential chirality. Crystal symmetry, the sites of the magnetic sublattice(s) and the nature of the frustration is given for each system. Additionally, the table also includes the paramagnetic Curie-Weiss parameters from fitted susceptibility, where available, as Weiss temperature and effective paramagnetic moment, θ_W and θ_{eff}. Negative $\theta_W < 0$ signifies dominating antiferromagnetic couplings, positive $\theta_W > 0$ gives ferromagnetic couplings. In the column on possible ground states, transition temperatures for Néel ordered states is given as T_N, otherwise absence of long-range order is indicated as "No LRO." If temperature maxima in the specific heat $C_p(T)$ have been observed, these are listed as T_{max}. If applicable, an estimated frustration parameter $f = |\theta_W|/T_{\text{max}}$ or $f = |\theta_W|/T_N$ is given.

System	Crystal symmetry	Magnetic sites	Magnetic sublattice	Paramagnetism Curie-Weiss fit: θ_W, μ_{eff}	Ground state transition temperature frustration parameter f	Reference(s)
$PbCuTe_2O_6$	$P4_132$ No. 213 Class O	$12d$ Cu^{2+}, $S = 1/2$	3D corner sharing triangles	−22 K, $1.73\mu_B$	Unknown $T^{\text{max}} = 1.15$ K $f = 19$	[54–56]
$Cu_2Te_2O_5X_2$ (X = Cl, Br)	$P\bar{4}$ Class S_4	$4h$ Cu^{2+}, $S = 1/2$	Irregular tetrahedra on square lattice	Susceptibility of isolated tetrahedral spin clusters	$T^{\text{max}} \sim 25$ K incommensurate possibly multi-k two propagation vectors, X = Cl; $T_N = 18$ K $k = (-x, y, 1/2)$, $k' = (x, y, 1/2)$ X = Br; $T_N = 11$ K	[57–59]
FeCrAs	$P\bar{6}2m$ No. 189 Class D_{3h}	Cr $3f$ Fe $3g$	Cr in distorted kagome layers Fe forms triangles	No Curie-Weiss	Only Cr orders $k = (1/3, 1/3, 0)$ $T_N \sim 125$ K Fe undetermined	[60–63]
$Bi_3Mn_4O_{12}(NO_3)$	$P3$ No. 143 Class C_3	Mn^{4+} $S = 3/2$ Mn1($1c$)Mn2($1b$) Mn3($1c$)Mn4($1b$)	Well separated, slightly distorted honeycomb layers	−257 K	$T_N < 0.4$ K, but with field induced spin order at higher T	[64,65]
$A(TiO)Cu_4(PO_4)_4$ (A = Ba, Pb, Sr)	$P42_12$ No. 90 Class D_4 chiral	Cu^{2+} $S = 1/2$ on $8g$	Corner sharing CuO_4 noncoplanar tetramers forming a square layer	A = Sr − 18 K, A = Pb − 22 K, A = Ba − 30 K, $1.9\mu_B$ A = Ba − 35 K, $1.97\mu_B$	Noncollinear Néel ordering $T_N = 6.1$ K (Sr) spin-nematic quadrupolar $f \sim 3$	[66–69]
$Ca_{10}Cr_7O_{28}$ Whitlockite type	$R3c$ No. 161 Class C_{3v}	Cr^{5+} $S = 1/2$ on $18b$ Cr^{6+} $S = 0$ on $6a$	Double-kagome layers	+2.35 K, $1.73\mu_B$	No LRO Spin liquid Possible field-induced magnetic ordering at high pressures.	[69–71]
$Na_4Ir_3O_8$	$P4_132$ No. 213 Class O chiral	Ir^{4+} $S = 1/2$ on $12d$	3D Hyperkagome lattice	−650 K, $1.96\mu_B$	No LRO above 2 K Spin liquid	[72]
$La_4Ru_6O_{19}$	$I23$ No. 197 Class T	$Ru^{+4.33}$ on $12e$ metallic	3D Shastry-Sutherland-like lattice	−14 K, $0.41\mu_B$	No LRO	[73,74]
LaIrSi-type intermetallic compounds	$P2_13$ No. 198 chiral	Rare-earth ions on La site $4a$	Trillium lattice		LaIrSi superconducting $T_C = 2.3$ K	[75,76]

(Table continued)

TABLE I. *(Continued)*

System	Crystal symmetry	Magnetic sites	Magnetic sublattice	Paramagnetism Curie-Weiss fit: θ_W, μ_{eff}	Ground state transition temperature frustration parameter f	Reference(s)
EuPtSi		Eu^{2+} $4a$ $S = 7/2$		7.7 K, $8.08\mu_B$	$T_N = 4.0$–4.1 K Incommensurate antiferromagnetic $k = (0.2, 0.3, 0)$ $f = 1.9$	[77–79]
CeIrSi		Ce^{3+} $4a$ $S = 1/2$		−21 K, $2.53\mu_B$	No LRO $T(\chi)^{\max} = 1.5$ K	[80]
$Ba_3Yb_2Zn_5O_{11}$ breathing pyrochlores	$\bar{4}3m$	Yb^{3+} $S = 1/2$ $J = 7/2$	Connected small and large tetrahedrons	−6.7 K	No LRO octupolar paramagnet	[81–83]
Swedenborgite-type magnets			Kagome with trigonal interstitial sites; see Fig. 1(a)			
$Y_{0.5}Ca_{0.5}BaCo_4O_7$	$P6_3mc$ ($P31c$, $Pna2_1$) No. 186 Class C_{6v}	Co^{2+} $2a, 6c$ $S = 3/2$ Co^{3+} $2a, 6c$ $S = 2$		−2200 K, $6.9\mu_B$	No LRO $f > 1000$ suppressed incommensurate	[34,51,52,84]
$YBaCo_3FeO_7$	$Pbn2_1$ No. 33 Magnetic structure $P112_1'$	Co^{2+} $4a$ $S = 3/2$ Co^{3+} $4a$ $S = 2$		−907 K, $2.23\mu_B$	$T_N = 110$ K $k = 0$ $f = 14$	[85]
$CaBaCo_3FeO_7$	$Pbn2_1$ No. 33 Magnetic structure $P112_1'$	Co^{2+} $4a$ $S = 3/2$ Co^{3+} $4a$ $S = 2$ Fe^{3+} 4a $S = 5/2$		−1400 K, $3.56\mu_B$	$T_N = 140$ K $k = (\frac{1}{3}, 0, 0)$ $f = 10$	[86]
$YBaCo_3FeO_7$	$P6_3mc$ No. 186 Class C_{6v}	Co^{2+} $2a, 6c$ $S = 3/2$ Fe^{3+} $2a, 6c$ $S = 5/2$		−2000 K, $3.63\mu_B$	Spin liquid $f > 1000$	[14] This work

closely resembles the evolution of $S(Q)$ [14] with temperature, which concurs with our observation of emerging chiral spin correlations. This behavior can be perceived as successive freezing of the spin system while retaining a liquidlike amorphous appearance without long-range order. In previous studies, it was speculated that this is a consequence of exchange disorder. In the single crystal study of $Y_{0.5}Ca_{0.5}BaCo_4O_7$ [52], excess oxygen seems to cause a lower symmetry $Pna2_1$ and, interestingly, suppressed incommensurate order is observed. In light of the present study, the common lack of long-range order may originate from a similar but yet hidden chirality.

The magnetism of the listed materials is diverse, containing magnetic oxides and metallic systems with 3d band magnetism or rare earths. This reflects the fact that only symmetry considerations dictate the presence of the chiral twisting exchange while the microscopic nature of the exchange itself is immaterial. The system $Ba_3Yb_2Zn_5O_{11}$ belongs to noncentrosymmetric breathing pyrocholore lattices from crystal class $\bar{4}3m$. It stands for a whole class of materials, where certain antiferromagnetic modes can couple via DM interaction, such that there Lifshitz(-type) invariants can arise in the phenomenological free energy, while they would not occur for simple ferromagnetic or antiferromagnetic ordering described by an axial vector. Hence, the particular frustrating role of the DM interaction in these systems depends on the details of the incipient antiferrromagnetic ordering. In particular, some of the systems are spin $S = 1/2$ quantum magnets. Also, in this case, the antisymmetric Dzyaloshinskii-Moriya exchange will result in textured states and the ground state could become a textured quantum spin liquid, where long-range quantum entanglement emerges on the background of localized or lumpy noncollinear spin patterns. For some systems with geometric frustration, e.g., $Na_4Ir_3O_8$ and $A(TiO)Cu_4(PO_4)_4$, with $A = Ba$, Sr, Pb, the possibility of multipolar ordering has been discussed, like spin-nematic quadrupolar states. The corresponding primary ordering modes then are not of dipolar type. But the twisting mechanism dictated by the acentric crystalline symmetry still exists. The corresponding multipolar textures then would be similar to the textures in chiral liquid crystals like cholesteric states of chiral nematics.

VI. CONCLUSIONS

To summarize, we have shown a first experimental evidence of a chiral spin liquid by polarized diffuse neutron scattering from a single domain crystal. Therefore, we used an advanced polarization analysis and established a method to separate and determine the full tensor of the chiral spin correlation function in real space by use of Fourier analysis. The particular chirality of cycloidal character with threefold symmetry links with the symmetry of the DM interactions that appear on the exchange path between kagome and interlayer sites. Therefore, the interlayer sites can be identified as the origin of the cycloidal waves spreading into the kagome planes. Within the surprisingly large observable range of correlations, the structure appears as an inhomogeneous magnetic state consisting of multiple of these zero-dimensional entities in a random rather than ordered fashion. The picture of this chiral lump pattern may resemble the wave pattern from a rain drop hitting a water surface, whereas the pattern of many rain drops results from a random superposition.

The stability of this short-range ordered state at low temperature is unexpected and imposes a fundamental challenge. Could this be explained in a classical picture based on the special role of DM interactions? Indeed, it is shown that the unavoidable antisymmetric DM exchange in this three-dimensional noncentrosymmetric magnetic system is able to prevent a classical ordering phase transition at finite temperature. The minimal assumptions for the mechanism in this spin system are (i) the existence of several nearly degenerate ordering modes, which is the rule in geometrically frustrated multisublattice antiferromagnets, and (ii) the existence of this chiral antisymmetric exchange. The avoidance of a standard classical phase transition into a long-range ordered state results from the violation of the Lifshitz criterion in the phenomenological Landau theory [35]. Instead, the frustration caused by the chiral DM exchange is able to cause the appearance of localized entities, static solitonic kinks, or skyrmion tubes, or ball-like objects, which we call "lumps," which is a general mechanism for chiral helimagnets with DM interactions [36,37]. The condensation of such entities into larger mesophases then is driven by different weaker forces. A prominent example for the condensation of spins into an inhomogeneous magnetic state is known for chiral helimagnets, the assembling of skyrmions into dense-packed lattices [38]. The impact of the DM interactions in polar crystal structure of $YBaCo_3FeO_7$ leads to the specific cycloidal twisting of spin patterns in directions within the hexagonal base plane. Based on symmetry considerations, we see that the spin system supports localized multiply twisted local spin objects, static solitons, with the shape and anisotropy of spin directions, in accordance with the chiral spin correlation observed in our experimental data. Extending this theory to describe the coupling of several ordering modes via the DM interactions, the analysis supports an anomalous magnetic ordering and the creation of a lumplike pattern of individual zero-dimensional entities. The theoretical concept relates to field theories for subnuclear particles. Such field theories, considering many order parameters and a static gauge field, allow for the presence of massive spatially extended lumps or static solitons [87,88]. The ordering of these entities into long-range ordered array may remain incomplete, as the frustration of the chiral couplings remains appreciable at

all scales, and the condensates may appear as amorphous textures. This means that the length scale related to the twisting of the primary ordering modes spatially limits the range of spin order, and no true phase transition between the paramagnetic state and the ground state takes place. A similar idea is used to describe the atomic short-range order of structural glasses where locally preferred clusters do not assemble into extended states [48]. In the limit of an ordering, described by infinitely many primary modes, the avoidance of true long-range order is exact [40]. This suggests that magnetic systems with many nearly degenerate ordering modes, such as geometrically frustrated antiferromagnets, do prefer to remain in an amorphous finite-temperature state, although they develop a correlated lumpy texture with a finite range.

The observation of chirality in a spin liquid has allowed us to identify a mechanism that exists in many frustrated acentric magnets and can be recognized by simple symmetry arguments. Crucial prerequisites, to obtain this twisted, lumplike short-range order, are frustrated spins with weak anisotropy that are easily rotatable by chiral exchange couplings. Of course, we exclude any noncompeting anisotropy, which arises from DM itself. Candidate materials for this type of chiral spin liquids and possible amorphous ground states are listed in Table I. The proposed mechanism may be the reason why these and further three-dimensional, frustrated, acentric magnets lack long-range spin ordering but exhibit exotic spin liquid states. Some of these systems order at finite temperatures, yet chiral twisted short-range order may still be observed by diffuse scattering above the ordering transition, e.g., the skyrmion precursor states in MnSi [49,50].

ACKNOWLEDGMENTS

This work is based on experiments performed at the DNS instrument operated by JCNS at the Heinz-Maier-Leibnitz Zentrum (MLZ), Garching, Germany. W. S. gratefully acknowledges Y. Su for supporting the experiments, and I. Heimbach and A. Müller from the Forschungszentrum Jülich for graphical support and data visualization. O. Zaharko, Y. Su, P. Manuel, T. Brückel, and J. van den Brink are acknowledged for useful comments and reading of the manuscript.

[1] J. Knolle and R. Moessner, *A Field Guide to Spin Liquids*, Annu. Rev. Condens. Matter Phys. **10**, 451 (2019).
[2] C. Castelnovo, R. Moessner, and S. L. Sondhi, *Spin Ice, Fractionalization, and Topological Order*, Annu. Rev. Condens. Matter Phys. **3**, 35 (2012).
[3] L. Balents, *Spin Liquids in Frustrated Magnets*, Nature (London) **464**, 199 (2010).
[4] J. Villain, R. Bidaux, J. P. Carton, and R. Conte, *Order as an Effect of Disorder*, J. Phys. (Paris) **41**, 1263 (1980).
[5] P. Santini, S. Carretta, G. Amoretti, R. Caciuffo, N. Magnani, and G. H. Lander, *Multipolar Interactions in f-Electron Systems: The Paradigm of Actinide Dioxides*, Rev. Mod. Phys. **81**, 807 (2009).
[6] J. A. M. Paddison, H. Jacobsen, O. A. Petrenko, M. T. Fernandez-Diaz, P. P. Deen, and A. L. Goodwin, *Hidden Order in Spin-Liquid* $Gd_3Ga_5O_{12}$, Science **350**, 179 (2015).
[7] S. T. Bramwell and M. J. P. Gingras, *Spin Ice State in Frustrated Magnetic Pyrochlore Materials*, Science **294**, 1495 (2001).
[8] Z. Y. Zhu, P. A. Maksimov, S. R. White, and A. L. Chernyshev, *Disorder-Induced Mimicry of a Spin Liquid in* $YbMgGaO_4$, Phys. Rev. Lett. **119**, 157201 (2017).
[9] X. G. Wen, *Topological Orders and Edge Excitations in Fractional Quantum Hall States*, Adv. Phys. **44**, 405 (1995).
[10] L. Savary and L. Balents, *Quantum Spin Liquids: A Review*, Rep. Prog. Phys. **80**, 016502 (2017).
[11] A. Szasz, J. Motruk, M. P. Zaletel, and J. E. Moore, *Chiral Spin Liquid Phase of the Triangular Lattice Hubbard Model: A Density Matrix Renormalization Group Study*, Phys. Rev. X **10**, 021042 (2020).
[12] G. Aminoff, *On a New Mineral from Langban*, Z. Kristallogr. **60**, 262 (1924).
[13] M. Valldor and M. Andersson, *The Structure of the New Compound* $YBaCo_3FeO_7$ *with a Magnetic Feature*, Solid State Sci. **4**, 923 (2002).
[14] M. Valldor, R. P. Hermann, J. Wuttke, M. Zamponi, and W. Schweika, *Spin Correlations in the Extended Kagome System* $YBaCo_3FeO_7$, Phys. Rev. B **84**, 224426 (2011).
[15] J. D. Reim, E. Rosen, W. Schweika, M. Meven, N. R. Leo, D. Meier, M. Fiebig, M. Schmidt, C. Y. Kuo, T. W. Pi, Z. Hu, and M. Valldor, *Structural Invariance upon Antiferromagnetic Ordering in Geometrically Frustrated Swedenborgite,* $CaBaCo_2Fe_2O_7$, J. Appl. Crystallogr. **47**, 2038 (2014).
[16] J. D. Reim, E. Rosen, O. Zaharko, M. Mostovoy, J. Robert, M. Valldor, and W. Schweika, *Neutron Diffraction Study and Theoretical Analysis of the Antiferromagnetic Order and the Diffuse Scattering in the Layered Kagome System* $CaBaCo_2Fe_2O_7$, Phys. Rev. B **97**, 144402 (2018).
[17] P. Manuel, L. C. Chapon, P. G. Radaelli, H. Zheng, and J. F. Mitchell, *Magnetic Correlations in the Extended Kagome* $YBaCo_4O_7$ *Probed by Single-Crystal Neutron Scattering*, Phys. Rev. Lett. **103**, 037202 (2009).
[18] D. D. Khalyavin, P. Manuel, J. F. Mitchell, and L. C. Chapon, *Spin Correlations in the Geometrically Frustrated* $RBaCo_4O_7$ *Antiferromagnets: Mean-Field Approach and Monte Carlo Simulations*, Phys. Rev. B **82**, 094401 (2010).
[19] S. Buhrandt and L. Fritz, *Spin-Liquid Phase and Order by Disorder of Classical Heisenberg Spins on the Swedenborgite Lattice*, Phys. Rev. B **90**, 020403(R) (2014).
[20] D. D. Khalyavin, P. Manuel, and L. C. Chapon, *Possible Chiral Spin-Liquid Phase in Noncentrosymmetric* $RBaCo_4O_7$, Phys. Rev. B **85**, 220401(R) (2012).
[21] T. Moriya, *Anisotropic Superexchange Interaction and Weak Ferromagnetism*, Phys. Rev. **120**, 91 (1960).
[22] F. Keffer, *Moriya Interaction and the Problem of the Spin Arrangements in β-MnS*, Phys. Rev. **126**, 896 (1962).

[23] M. Valldor and O. Breunig, *Crystal Structure and Properties of the Manganese Containing Swedenborgite* $YBaMn_3AlO_7$, Solid State Sci. **13**, 831 (2011).

[24] M. Valldor, *Syntheses and Structures of Compounds with* $YBaCo_3FeO_7$*-Type Structure*, Solid State Sci. **6**, 251 (2004).

[25] M. Karppinen, H. Yamauchi, S. Otani, T. Fujita, T. Motohashi, Y. H. Huang, M. Valkeapaa, and H. Fjellvag, *Oxygen Nonstoichiometry in* $YBaCo_4O_{7+\delta}$*: Large Low-Temperature Oxygen Absorption/Desorption Capability*, Chem. Mater. **18**, 490 (2006).

[26] E. V. Tsipis, V. V. Kharton, J. R. Frade, and P. Nunez, *High-Temperature Transport and Electrochemical Properties of* $YBaCo_4O_{7+\delta}$, J. Solid State Electrochem. **9**, 547 (2005).

[27] S. Kadota, M. Karppinen, T. Motohashi, and H. Yamauchi, *R-Site Substitution Effect on the Oxygen-Storage Capability of* $RBaCo_4O_{7+\delta}$, Chem. Mater. **20**, 6378 (2008).

[28] O. Chmaissem, H. Zheng, A. Huq, P. W. Stephens, and J. F. Mitchell, *Formation of* Co^{3+} *Octahedra and Tetrahedra in* $YBaCo_4O_{8.1}$, J. Solid State Chem. **181**, 664 (2008).

[29] W. Schweika, *XYZ-Polarisation Analysis of Diffuse Magnetic Neutron Scattering from Single Crystals*, J. Phys. Conf. Ser. **211**, 012026 (2010).

[30] O. Schärpf and H. Capellmann, *The XYZ-Difference Method with Polarized Neutrons and the Separation of Coherent, Spin Incoherent, and Magnetic Scattering Cross-Sections in a Multidetector*, Phys. Status Solidi A **135**, 359 (1993).

[31] M. Blume, *Polarization Effects in Magnetic Elastic Scattering of Slow Neutrons*, Phys. Rev. **130**, 1670 (1963).

[32] S. V. Maleev, V. G. Baryakhtar, and R. A. Suris, *The Scattering of Slow Neutrons by Complex Magnetic Structures*, Sov. Phys. Solid State **4**, 2533 (1963).

[33] W. Schweika, *Disordered Alloys: Diffuse Scattering and Monte Carlo Simulations* (Springer-Verlag, Berlin, 1998).

[34] J. R. Stewart, G. Ehlers, H. Mutka, P. Fouquet, C. Payen, and R. Lortz, *Spin Dynamics, Short-Range Order, and Spin Freezing in* $Y_{0.5}Ca_{0.5}BaCo_4O_7$, Phys. Rev. B **83**, 024405 (2011).

[35] J. C. Tolédano and P. Tolédano, *The Landau Theory of Phase Transitions Application to Structural, Incommensurate, Magnetic and Liquid Crystal Systems* (World Scientific, Singapore, 1987).

[36] A. N. Bogdanov and D. A. Yablonsky, *Thermodynamically Stable Vortexes in Magnetically Ordered Crystals. The Mixed State of Magnetics*, Zh. Eksp. Teor. Fiz. **95**, 178 (1989) [JETP, 68, 101 (1989)], http://www.jetp.ras.ru/cgi-bin/dn/e_068_01_0101.pdf.

[37] A. Bogdanov, *New Localized Solutions of the Nonlinear Field-Equations*, JETP Lett. **62**, 247 (1995).

[38] U. K. Rößler, A. N. Bogdanov, and C. Pfleiderer, *Spontaneous Skyrmion Ground States in Magnetic Metals*, Nature (London) **442**, 797 (2006).

[39] I. E. Dzyaloshinskii, *Theory of Helicoidal Structures in Antiferromagnets. I. Nonmetals*, Sov. Phys. JETP **19**, 960 (1964).

[40] Z. Nussinov, *Avoided Phase Transitions and Glassy Dynamics in Geometrically Frustrated Systems and Non-Abelian Theories*, Phys. Rev. B **69**, 014208 (2004).

[41] S. Elitzur, *Impossibility of Spontaneously Breaking Local Symmetries*, Phys. Rev. D **12**, 3978 (1975).

[42] C. D. Batista and Z. Nussinov, *Generalized Elitzur's Theorem and Dimensional Reductions*, Phys. Rev. B **72**, 045137 (2005).

[43] J. A. Hertz, *Gauge Models for Spin-Glasses*, Phys. Rev. B **18**, 4875 (1978).

[44] J. Greensite and K. Matsuyama, *Higgs Phase as a Spin Glass and the Transition between Varieties of Confinement*, Phys. Rev. D **101**, 054508 (2020).

[45] F. R. Klinkhamer and N. S. Manton, *A Saddle-Point Solution in the Weinberg-Salam Theory*, Phys. Rev. D **30**, 2212 (1984).

[46] N. S. Manton, *The Inevitability of Sphalerons in Field Theory*, Phil. Trans. R. Soc. A **377**, 20180327 (2019).

[47] C. H. Taubes, *The Existence of a Non-Minimal Solution to the SU(2) Yang-Mills-Higgs Equations on* $\mathbb{R}^3$. *Part I*, Commun. Math. Phys. **86**, 257 (1982).

[48] J.-F. Sadoc and R. Mosseri, *Geometrical Frustration* (Cambridge University Press, Cambridge, England, 1999).

[49] C. Pappas, E. Lelievre-Berna, P. Falus, P. M. Bentley, E. Moskvin, S. Grigoriev, P. Fouquet, and B. Farago, *Chiral Paramagnetic Skyrmion-like Phase in MnSi*, Phys. Rev. Lett. **102**, 197202 (2009).

[50] H. Wilhelm, M. Baenitz, M. Schmidt, U. K. Rößler,, A. A. Leonov, and A. N. Bogdanov, *Precursor Phenomena at the Magnetic Ordering of the Cubic Helimagnet FeGe*, Phys. Rev. Lett. **107**, 127203 (2011).

[51] W. Schweika, M. Valldor, and P. Lemmens, *Approaching the Ground State of the Kagome Antiferromagnet*, Phys. Rev. Lett. **98**, 067201 (2007).

[52] S. Gao, V. Kocsis, M. Soda, F. Ye, Y. Liu, A. F. May, Y. Taguchi, Y. Tokura, T.-H. Arima, W. Schweika, M. B. Stone, and A. D. Christianson, *Suppressed Incommensurate Order in the Swedenborgite* $Ca_{0.5}Y_{0.5}BaCo_4O_7$, Phys. Rev. B **104**, L140408 (2021).

[53] M. Iakovleva, S. Zimmermann, J. Zeisner, A. Alfonsov, H.-J. Grafe, M. Valldor, E. Vavilova, B. Büchner, and V. Kataev, *Magnetic Resonance Spectroscopy on the Spin-Frustrated Magnets* $YBaCo_3MO_7$ *(*M = Al*, Fe)*, Phys. Rev. B **96**, 064417 (2017).

[54] B. Koteswararao, R. Kumar, P. Khuntia, S. Bhowal, S. K. Panda, M. R. Rahman, A. V. Mahajan, I. Dasgupta, M. Baenitz, K. H. Kim, and F. C. Chou, *Magnetic Properties and Heat Capacity of the Three-Dimensional Frustrated* $S = 1/2$ *Antiferromagnet* $PbCuTe_2O_6$, Phys. Rev. B **90**, 035141 (2014).

[55] P. Khuntia, F. Bert, P. Mendels, B. Koteswararao, A. V. Mahajan, M. Baenitz, F. C. Chou, C. Baines, A. Amato, and Y. Furukawa, *Spin Liquid State in the 3D Frustrated Antiferromagnet* $PbCuTe_2O_6$*: NMR and Muon Spin Relaxation Studies*, Phys. Rev. Lett. **116**, 107203 (2016).

[56] S. Chillal, Y. Iqbal, H. O. Jeschke, J. A. Rodriguez-Rivera, R. Bewley, P. Manuel, D. Khalyavin, P. Steffens, R. Thomale, A. T. M. N. Islam, J. Reuther, and B. Lake, *Evidence for a Three-Dimensional Quantum Spin Liquid in* $PbCuTe_2O_6$, Nat. Commun. **11**, 2348 (2020).

[57] M. Johnsson, K. W. Tornroos, F. Mila, and P. Millet, *Tetrahedral Clusters of Copper(II): Crystal Structures and Magnetic Properties of* $Cu_2Te_2O_5X_2$ *(*X = Cl*, Br)*, Chem. Mater. **12**, 2853 (2000).

[58] O. Zaharko, A. Daoud-Aladine, S. Streule, J. Mesot, P. J. Brown, and H. Berger, *Incommensurate Magnetic Ordering in* $Cu_2Te_2O_5X_2$ *(X = Cl, Br) Studied by Neutron Diffraction*, Phys. Rev. Lett. **93**, 217206 (2004).

[59] O. Zaharko, H. Ronnow, J. Mesot, S. J. Crowe, D. M. Paul, P. J. Brown, A. Daoud-Aladine, A. Meents, A. Wagner, M. Prester, and H. Berger, *Incommensurate Magnetic Ordering in* $Cu_2Te_2O_5X_2$ *(X = Cl, Br) Studied by Single Crystal Neutron Diffraction*, Phys. Rev. B **73**, 064422 (2006).

[60] A. Akrap, Y. M. Dai, W. Wu, S. R. Julian, and C. C. Homes, *Optical Properties and Electronic Structure of the Nonmetallic Metal FeCrAs*, Phys. Rev. B **89**, 125115 (2014).

[61] W. Wu, A. McCollam, I. Swainson, P. M. C. Rourke, D. G. Rancourt, and S. R. Julian, *A Novel Non-Fermi-Liquid State in the Iron-Pnictide FeCrAs*, Europhys. Lett. **85**, 17009 (2009).

[62] I. P. Swainson, W. L. Wu, A. McCollam, and S. R. Julian, *Non-Collinear Antiferromagnetism in FeCrAs*, Can. J. Phys. **88**, 701 (2010).

[63] B. M. Huddart, M. T. Birch, F. L. Pratt, S. J. Blundell, D. G. Porter, S. J. Clark, W. Wu, S. R. Julian, P. D. Hatton, and T. Lancaster, *Local Magnetism, Magnetic Order and Spin Freezing in the 'Nonmetallic Metal' FeCrAs*, J. Phys. Condens. Matter **31**, 285803 (2019).

[64] O. Smirnova, M. Azuma, N. Kumada, Y. Kusano, M. Matsuda, Y. Shimakawa, T. Takei, Y. Yonesaki, and N. Kinomura, *Synthesis, Crystal Structure, and Magnetic Properties of* $Bi_3Mn_4O_{12}(NO_3)$ *Oxynitrate Comprising* $S = 3/2$ *Honeycomb Lattice*, J. Am. Chem. Soc. **131**, 8313 (2009).

[65] M. Matsuda, M. Azuma, M. Tokunaga, Y. Shimakawa, and N. Kumada, *Disordered Ground State and Magnetic Field-Induced Long-Range Order in an* $S = 3/2$ *Antiferromagnetic Honeycomb Lattice Compound* $Bi_3Mn_4O_{12}(NO_3)$, Phys. Rev. Lett. **105**, 187201 (2010).

[66] K. Kimura, M. Sera, and T. Kimura, $A(2+)$ *Cation Control of Chiral Domain Formation in* $A(TiO)Cu_4(PO_4)_4$ *(A = Ba, Sr)*, Inorg. Chem. **55**, 1002 (2016).

[67] P. Babkevich, L. Testa, K. Kimura, T. Kimura, G. S. Tucker, B. Roessli, and H. M. Ronnow, *Magnetic Structure of* $Ba(TiO)Cu_4(PO_4)_4$ *Probed Using Spherical Neutron Polarimetry*, Phys. Rev. B **96**, 214436 (2017).

[68] K. Kimura, M. Toyoda, P. Babkevich, K. Yamauchi, M. Sera, V. Nassif, H. M. Ronnow, and T. Kimura, *A-Cation Control of Magnetoelectric Quadrupole Order in* $A(TiO)Cu_4(PO_4)_4$ *(A = Ba, Sr, and Pb)*, Phys. Rev. B **97**, 134418 (2018).

[69] V. Kumar, A. Shahee, S. Kundu, M. Baenitz, and A. V. Mahajan, *The Spin-1/2 Coupled Tetramer System* $Ba(TiO)Cu_4(PO_4)_4$ *Probed by Magnetization, Specific Heat, and* ^{31}P*-NMR*, J. Magn. Magn. Mater. **492**, 165600 (2019).

[70] C. Balz, B. Lake, M. Reehuis, A. T. M. N. Islam, O. Prokhnenko, Y. Singh, P. Pattison, and S. Toth, *Crystal Growth, Structure and Magnetic Properties of* $Ca_{10}Cr_7O_{28}$, J. Phys. Condens. Matter **29**, 225802 (2017).

[71] A. Balodhi and Y. Singh, *Synthesis and Pressure and Field-Dependent Magnetic Properties of the Kagome-Bilayer Spin Liquid* $Ca_{10}Cr_7O_{28}$, Phys. Rev. Mater. **1**, 024407 (2017).

[72] Y. Okamoto, M. Nohara, H. Aruga-Katori, and H. Takagi, *Spin-Liquid State in the* $S = 1/2$ *Hyperkagome Antiferromagnet* $Na_4Ir_3O_8$, Phys. Rev. Lett. **99**, 137207 (2007).

[73] P. Khalifah, K. D. Nelson, R. Jin, Z. Q. Mao, Y. Liu, Q. Huang, X. P. A. Gao, A. P. Ramirez, and R. J. Cava, *Non-Fermi-Liquid Behaviour in* $La_4Ru_6O_{19}$, Nature (London) **411**, 669 (2001).

[74] Y. A. Ying, K. D. Nelson, I. G. Deac, P. Schiffer, P. Khalifah, R. J. Cava, and Y. Liu, *Possible Observation of Quantum Ferromagnetic Fluctuations in* $La_4Ru_6O_{19}$, Phys. Rev. B **80**, 024303 (2009).

[75] B. Chevalier, P. Lejay, A. Cole, M. Vlasse, and J. Etourneau, *Crystal-Structure, Superconducting and Magnetic-Properties of New Ternary Silicides LaRhSi, LaIrSi and NdIrSi*, Solid State Commun. **41**, 801 (1982).

[76] B. Heying, R. Pottgen, M. Valldor, U. C. Rodewald, R. Mishra, and R. D. Hoffmann, *Synthesis, Structure, and Magnetic Properties of the Silicides RE*IrSi *(RE = Ce, Pr, Er, Tm, Lu) and* $SmIr_{0.266(8)}Si_{1.734(8)}$, Monatsh. Chem. **135**, 1335 (2004).

[77] M. Kakihana, D. Aoki, A. Nakamura, F. Honda, M. Nakashima, Y. Amako, S. Nakamura, T. Sakakibara, M. Hedo, T. Nakama, and Y. Onuki, *Giant Hall Resistivity and Magnetoresistance in Cubic Chiral Antiferromagnet EuPtSi*, J. Phys. Soc. Jpn. **87**, 023701 (2018).

[78] T. Sakakibara, S. Nakamura, S. Kittaka, M. Kakihana, M. Hedo, T. Nakama, and Y. Onuki, *Fluctuation-Induced First-Order Transition and Tricritical Point in EuPtSi*, J. Phys. Soc. Jpn. **88**, 093701 (2019).

[79] K. Kaneko, M. D. Frontzek, M. Matsuda, A. Nakao, K. Munakata, T. Ohhara, M. Kakihana, Y. Haga, M. Hedo, T. Nakama, and Y. Onuki, *Unique Helical Magnetic Order and Field-Induced Phase in Trillium Lattice Antiferromagnet EuPtSi*, J. Phys. Soc. Jpn. **88**, 013702 (2019).

[80] F. Kneidinger, I. Zeiringer, A. Siderenko, E. Bauer, H. Michor, P. Rogl, and J. G. Sereni, *Physical Properties of CeIrSi with Trillium-Lattice Frustrated Magnetism*, Phys. Rev. B **100**, 134442 (2019).

[81] K. Kimura, S. Nakatsuji, and T. Kimura, *Experimental Realization of a Quantum Breathing Pyrochlore Antiferromagnet*, Phys. Rev. B **90**, 060414(R) (2014).

[82] J. G. Rau, L. S. Wu, A. F. May, L. Poudel, B. Winn, V. O. Garlea, A. Huq, P. Whitfield, A. E. Taylor, M. D. Lumsden, M. J. P. Gingras, and A. D. Christianson, *Anisotropic Exchange within Decoupled Tetrahedra in the Quantum Breathing Pyrochlore* $Ba_3Yb_2Zn_5O_{11}$, Phys. Rev. Lett. **116**, 257204 (2016).

[83] T. Haku, K. Kimura, Y. Matsumoto, M. Soda, M. Sera, D. Yu, R. A. Mole, T. Takeuchi, S. Nakatsuji, Y. Kono, T. Sakakibara, L. J. Chang, and T. Masuda, *Low-Energy Excitations and Ground-State Selection in the Quantum Breathing Pyrochlore Antiferromagnet* $Ba_3Yb_2Zn_5O_{11}$, Phys. Rev. B **93**, 220407(R) (2016).

[84] M. Valldor, *Remnant Magnetization Above Room Temperature in the Semiconductor* $Y_{0.5}Ca_{0.5}BaCo_4O_7$, Solid State Sci. **8**, 1272 (2006).

[85] L. C. Chapon, P. G. Radaelli, H. Zheng, and J. F. Mitchell, *Competing Magnetic Interactions in the Extended Kagome System* $YBaCo_3FeO_7$, Phys. Rev. B **74**, 172401 (2006).

[86] N. Qureshi, M. T. Fernandez Diaz, L. C. Chapon, A. Senyshyn, W. Schweika, and M. Valldor, *Magnetic Structure of the Swedenborgite* $CaBa(Co_3Fe)O_7$ *Derived by Unpolarized Neutron Diffraction and Spherical Neutron Polarimetry*, Phys. Rev. B **97**, 064404 (2018).

[87] L. D. Faddeev, *Some Comments on Many-Dimensional Solitons*, Lett. Math. Phys. **1**, 289 (1976).

[88] S. Coleman, *New Phenomena in Subnuclear Physics* (Springer, Boston, MA, 1977), pp. 297–421.